Antiviral Research 140 (2017) 1–12

Contents lists available at ScienceDirect

Antiviral Research

journal homepage: www.elsevier.com/locate/antiviral

Biological or pharmacological activation of protein kinase C alpha constrains hepatitis E virus replication

Wenshi Wang [a], Yijin Wang [a], Yannick Debing [b], Xinying Zhou [a], Yuebang Yin [a], Lei Xu [a], Elena Herrera Carrillo [c], Johannes H. Brandsma [d], Raymond A. Poot [d], Ben Berkhout [c], Johan Neyts [b], Maikel P. Peppelenbosch [a], Qiuwei Pan [a, *]

[a] Department of Gastroenterology and Hepatology, Postgraduate School Molecular Medicine, Erasmus MC, University Medical Center, Rotterdam, The Netherlands
[b] Department of Microbiology and Immunology, Rega Institute for Medical Research, KU Leuven, Leuven, Belgium
[c] Laboratory of Experimental Virology, Department of Medical Microbiology, Center for Infection and Immunity Amsterdam (CINIMA), Academic Medical Center of the University of Amsterdam, Amsterdam, The Netherlands
[d] Department of Cell Biology, Medical Genetics Cluster, Erasmus MC, Rotterdam, The Netherlands

ARTICLE INFO

Article history:
Received 24 October 2016
Received in revised form
4 January 2017
Accepted 6 January 2017
Available online 8 January 2017

Keywords:
PKCα
Hepatitis E virus
PMA
AP-1
ISG

ABSTRACT

Although hepatitis E has emerged as a global health issue, there is limited knowledge of its infection biology and no FDA-approved medication is available. Aiming to investigate the role of protein kinases in hepatitis E virus (HEV) infection and to identify potential antiviral targets, we screened a library of pharmacological kinase inhibitors in a cell culture model, a subgenomic HEV replicon containing luciferase reporter. We identified protein kinase C alpha (PKCα) as an essential cell host factor restricting HEV replication. Both specific inhibitor and shRNA-mediated knockdown of PKCα enhanced HEV replication. Conversely, over-expression of the activated form of PKCα or treatment with its pharmacological activator strongly inhibited HEV replication. Interestingly, upon the stimulation by its activator, PKCα efficiently activates its downstream Activator Protein 1 (AP-1) pathway, leading to the induction of antiviral interferon-stimulated genes (ISGs). This process is independent of the JAK-STAT machinery and interferon production. However, PKCα induced HEV inhibition appears independent of the AP1 cascade. The discovery that activated PKCα restricts HEV replication reveals new insight of HEV-host interactions and provides new target for antiviral drug development.

1. Introduction

Hepatitis E virus (HEV) is one of the most common causes of acute viral hepatitis in the world. Although the mortality rate is <1% among the general population, pregnant women can have a fatality rate of up to 30% (Hakim et al., 2017). Additionally, chronic hepatitis E has become a significant clinical problem in immunocompromised patients. Up to date, there is still no proven medication available and its infection biology is poorly understood.

Protein kinases are principal components of the machineries that orchestrate immune response against diverse pathogenic entities, including viruses, by subsequent stimulation of specific signal transduction cascades (Lupberger et al., 2011). However, kinase controlled pathways employed by the host cells to stimulate antiviral immunity remain largely obscure. Knowledge of such pathways could prove exceedingly useful for the rational design of therapeutic avenues against HEV infection.

Encouragingly, numerous pharmacological kinase inhibitors or activators have been developed to target particular kinases. Among those, several are approved drugs in particular for treating cancer (Llovet et al., 2008), and many are currently at various stages of preclinical and clinical development. These compounds have broad implications for treating various diseases, including cancer, inflammation, diabetes and viral infections (Rask-Andersen et al., 2014; Zhang et al., 2009).

Thus, this study aims to comprehensively profile kinase-mediated cascades in cell–autonomous antiviral immunity starting from screening a library of pharmacological kinase inhibitors in

* Corresponding author. Department of Gastroenterology and Hepatology, Erasmus MC, Room Na-617, 's-Gravendijkwal 230, NL-3015 CE, Rotterdam, The Netherlands.
E-mail address: q.pan@erasmusmc.nl (Q. Pan).

http://dx.doi.org/10.1016/j.antiviral.2017.01.005
0166-3542/

Huh7 based HEV replication cell model. We identified protein kinase C alpha (PKCα) as an important anti-HEV mediator. Concurrently, we also revealed a novel function of PKC-Activator Protein 1 (AP-1) pathway, serving as a non-canonical pathway to activate transcription of antiviral interferon-stimulated genes (ISGs).

2. Materials and methods

2.1. Reagents and antibodies

Stocks of phorbol 12-myristate 13-acetate (PMA) (Sigma-Aldrich, St Louis, MO) and JAK inhibitor I (Santa Cruz Biotech, Santa Cruz, CA) were dissolved in dimethyl sulfoxide (DMSO) (Sigma-Aldrich, St Louis, MO) to concentrations of 100 μg/ml and 20 mM, respectively. Antibodies including phospho-PKCα/β (#9375), phospho-STAT1 (58D6, #9167), c-Fos (9F6, #2250), RelA (C22B4, #4764), Anti-rabbit IgG(H+L),F(ab') 2 Fragment (Alexa Fluor 488 conjugate) and Anti-mouse IgG (H+L), F(ab')2 Fragment (Alexa Fluor® 488 Conjugate) were purchased from Cell Signaling Technology, the Netherlands. Anti-rabbit or anti-mouse IRDye-conjugated antibodies were used as secondary antibodies for western blotting (Stressgen, Victoria, BC, Canada).

2.2. Viruses and cell culture models

Hepatocellular carcinoma cells Huh7 were kindly provided by Professor Bart Haagmans from Department of Viroscience, Erasmus Medical Center. Human Embryonic Kidney 293 cells were originally obtained from ATCC (www.atcc.org). The HEV infectious model (Huh7-P6) was based on Huh7 cells containing the full-length HEV genome (Kernow-C1 p6 clone, GenBank Accession Number JQ679013) (Wang et al., 2016a). Infectious HEV particles are generated and secreted into cell culture medium, which can be collected and used for secondary infection (Shukla et al., 2011, 2012; Wang et al., 2014; Zhou et al., 2014). The HEV subgenomic model was based on Huh7 cells containing the subgenomic HEV sequence (Kernow-C1 p6/luc) coupled to a Gaussia luciferase reporter gene. HEV replication defective model was based on Huh7 cells transfected with *in vitro* transcribed RNA from MluI-linearized plasmids p6-luc-GAD (kindly provided by Suzanne U. Emerson). A mutation in the HEV polymerase results in defect of viral replication. ISRE, NF-κB, AP-1 luciferase reporter cells were generated by transducing Huh7 cells with lentiviral vectors expressing the firefly luciferase gene under the control of ISRE, NF-κB, AP-1 promoters, respectively (System Biosciences). For simian rotavirus, SA11, a well-characterized and broadly used laboratory strain, was used to inoculate the Caco2 cell line as a rotavirus infection model. Murine norovirus 1 (MNV-1) was used to infect RAW 264.7 cells as a norovirus infection model (Wobus et al., 2004). The HIV virus production model was based on 293T cells transfected with HIV-1 molecular clone pLAI and pRL. The HIV single cycle entry model was based on TZM-bl cells infected with HIV clone Plai (van Bel et al., 2014). For influenza virus, multicycle replication curves were generated by inoculating A549 cells at a multiplicity of infection (MOI) of 0.01 50 percent tissue culture infectious doses ($TCID_{50}$) of A/Netherlands/246/1978(A/H3N2) or A/Netherlands/602/09 (A/H1N1) in duplicate. Supernatants were sampled at 0, 6, 12, 24, 48 and 72 h post inoculation, and virus titers in these supernatants were determined by means of end-point titration in MDCK cells as described previously (Schrauwen et al., 2013).

2.3. Screen of pharmacological kinase inhibitors

The kinase inhibitor library used for the screening was made available by the KU Leuven Centre for Drug Design & Development (www.cd3.eu). Huh7 cells were seeded in 96-well plates at 7.5×10^3 cells per well in 100 μl of DMEM with10% FBS and were incubated at 37 °C. After 24 h, cell layers were washed and transfected with capped p6/luc RNA (100 ng per well [each]) by use of DMRIE-C reagent (0.2 μl per well) according to the manufacturer's instructions. Plates were incubated at 37 °C for 4 h. Afterwards, the transfection medium was removed. Cell layers were washed twice with PBS and 100 μl of compound (diluted to a final concentration of 100, 20, 4 and 0.8 μM, respectively, in DMEM with 10% FBS) was added to each well. For control wells, the compound was omitted. After incubation for 3 days, HEV replicon − related Gaussia luciferase values were measured accordingly (Debing et al., 2014). Cell viability (CV) caused by compound-specific side effects were also analyzed after 3 days by using the CellTiter 96 AQ_{ueous} nonradioactive cell proliferation (monotetrazolium salt [MTS]) assay (Promega) (de Wilde et al., 2014). HEV replicon - related luciferase values were normalized with the following formula: $Luc\ (Norm) = (Luc_{\ replicon\ +\ compound} - Luc_{\ replicon\ +\ control})/(CV_{\ replicon\ +\ compound} - CV_{\ replicon\ +\ control})$.

2.4. Gene knockdown or over-expression by lentiviral vectors

Lentiviral pLKO knockdown vectors (Sigma−Aldrich) targeting PKCα, PKCβ, IRF9, RelA, c-Fos or control were obtained from the Erasmus Biomics Center and produced in HEK293T cells as previously described (Pan et al., 2009). After a pilot study, the shRNA vectors exerting optimal gene knockdown were selected. These shRNA sequences are listed in Supplementary Table 2. Stable gene knockdown cells were generated after lentiviral vector transduction and puromycin (2.5 μg/ml; Sigma) selection. wtPKCα and caPKCα overexpression lentivral vectors were a kind gift from Dr. Lin from the University of Minnesota. To create stable overexpression cell lines, GFP positive cells were sorted by cell sorter after lentiviral vectors transduction.

2.5. Reinfection assays

Reinfection assay was performed accordingly (Xu et al., 2016). Supernatant (containing infectious HEV particles) was collected from Huh7-P6 HEV model and purified by ultracentrifugation. The supernatant was first filtered through 0.45 mm filter followed by centrifugation at 10,000 rpm for 30 min to remove cell debris and then 22,000 rpm for 2 h to pellet HEV virus (SW 28 rotor). The pellet was suspended and diluted to 1×10^7 HEV viral RNA copies/ml. The diluted HEV virus stock was stored at −80 °C. For HEV infection, cells were seeded into 12-well plates at a density of 7×10^4 cells per well and incubated for 24 h. Next, cells were incubated with 400 μl HEV stock (1×10^7 viral RNA copies/ml) per well at 37 °C for 6 h. Then, the inoculum was removed, and cell layers were washed 3 times with PBS, and 1 ml fresh medium was added to each well.

2.6. Measurement of luciferase activity

For Gaussia luciferase, the secreted luciferase activity in the cell culture medium was measured by BioLux® Gaussia Luciferase Flex Assay Kit (New England Biolabs). For firefly luciferase, luciferin potassium salt (100 mM; Sigma) was added to cells and incubated for 30 min at 37 °C. Both Gaussia and firefly luciferase activity was quantified with a LumiStar Optima luminescence counter (BMG LabTech, Offenburg, Germany).

2.7. Quantitative real-time polymerase chain reaction

RNA was isolated with a Machery-NucleoSpin RNA II kit (Bioke,

Leiden, The Netherlands) and quantified using a Nanodrop ND-1000 (Wilmington, DE, USA). cDNA was synthesized from total RNA using a cDNA Synthesis Kit (TAKARA BIO INC). The cDNA of all target genes was amplified for 50 cycles and quantified with a SYBRGreen-based real-time PCR (Applied Biosystems) according to the manufacturer's instructions. GAPDH was considered as a reference gene to normalize gene expression. Relative gene expression was normalized to GAPDH using the formula $2^{-\Delta\Delta CT}$ ($\Delta\Delta CT = \Delta CT_{sample} - \Delta CT_{control}$). All the primer sequences are included in Supplementary Table 3.

2.8. Western blot assay

Cultured cells were lysed in Laemmli sample buffer containing 0.1 M DTT and heated 5 min at 95 °C, followed by loading onto a 10% sodium dodecyl sulfate polyacrylamide gel and separation by electrophoresis. After 90 min running at 120 V, proteins were electrophoretically transferred onto a polyvinylidene difluoride membrane (Invitrogen) for 1.5 h with an electric current of 250 mA. Subsequently, the membrane was blocked with a mixture of 2.5 ml blocking buffer (Odyssey) and 2.5 ml phosphate-buffered saline containing 0.05% Tween 20. It was followed by overnight incubation with primary antibodies (1:1000) at 4 °C. The membrane was washed 3 times followed by incubation for 1 h with IRDye-conjugated secondary antibody (1:5000). After washing 3 times, protein bands were detected with the Odyssey 3.0 Infrared Imaging System.

2.9. Confocal laser electroscope assay

Huh7 cells were seeded on glass coverslips. After 12 h, cells were washed with PBS, fixed in 4% formalin for 10 min and blocked with tween-milk-glycine medium (PBS, 0.05% tween, 5 g/L skim milk and 1.5 g/L glycine). Samples were incubated with primary antibodies overnight at 4 °C. Subsequently, samples were incubated with 1:1000 dilutions of the anti-mouse IgG (H+L), F(ab')2 Fragment (Alexa Fluor® 488 Conjugate) or anti-rabbit IgG(H+L), F(ab') 2 Fragment (Alexa Fluor 488 conjugate) secondary antibodies. Nuclei were stained with DAPI (4,6-diamidino-2-phenylindole; Invitrogen). Images were detected using confocal electroscope.

2.10. Creation of mutant ISRE reporter cell line

Based on the sequence specific ISRE motif, a mutant version of ISRE was designed and synthesized (Forward: 5′-

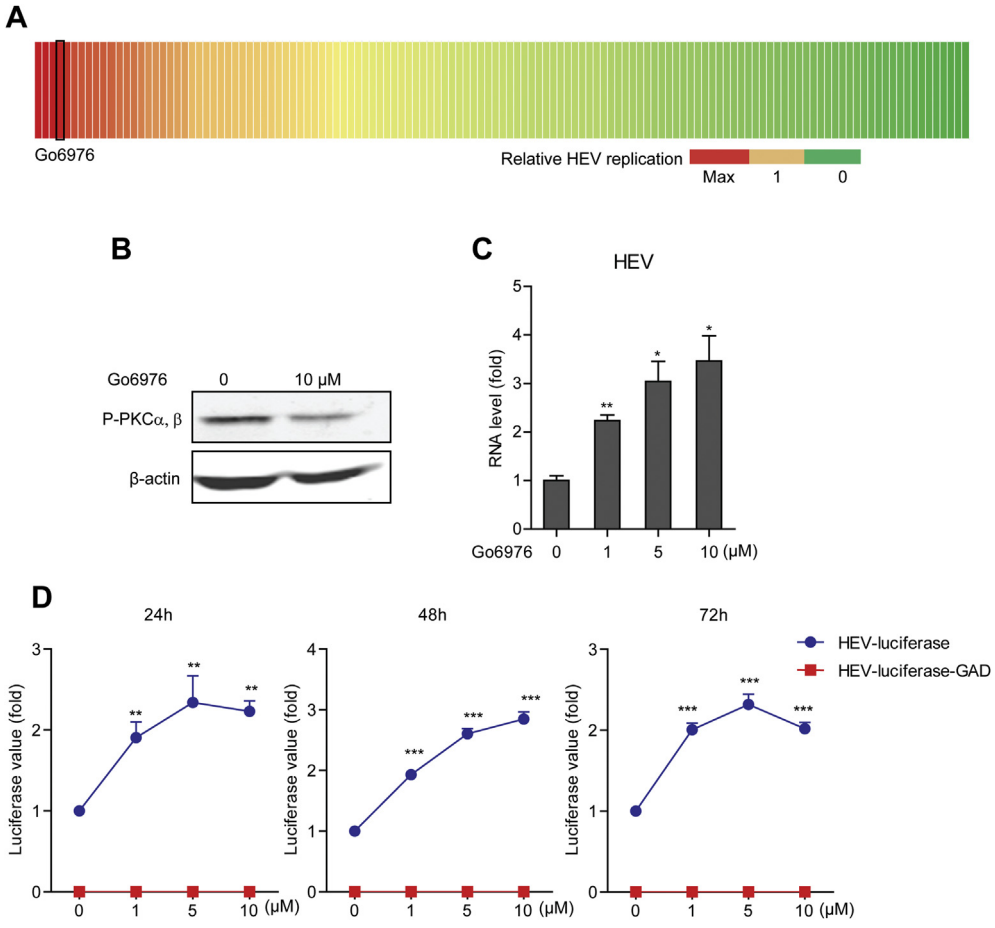

Fig. 1. Conventional PKCs function as cell-autonomous antiviral elements against HEV. (A) Heatmap summary of the screening results. The Huh7 cell line transfected with a subgenomic HEV luciferase reporter replicon was used. Compared to control, relative HEV luciferase activity depicted in red to green for each inhibitor. Red means that the signal is higher than control; whereas green means lower than control. See also Table S1. (B) Go6976 (10 μM) treatment inhibited phosphorylation of PKCα and PKCβ protein levels in Huh7 cells as determined by western blot. (C) qRT-PCR analysis of HEV RNA in Huh7 cells harboring full-length HEV infectious genome. Treatment with Go6976 increased cellular HEV RNA (n = 3). (D) In the Huh7 cell-based subgenomic HEV replicon model, treatment with different doses of Go6976 increased HEV replication-related luciferase activity. Cells transfected with replicon defective control (HEV-luciferase-GAD) RNA were also treated with Go6976 (n = 3 independent experiments with 2–3 replicates each). Data presented as mean ± SEM (*, $P < 0.05$; **, $P < 0.01$; ***, $P < 0.001$; ns, not significant). (For interpretation of the references to colour in this figure legend, the reader is referred to the web version of this article.)

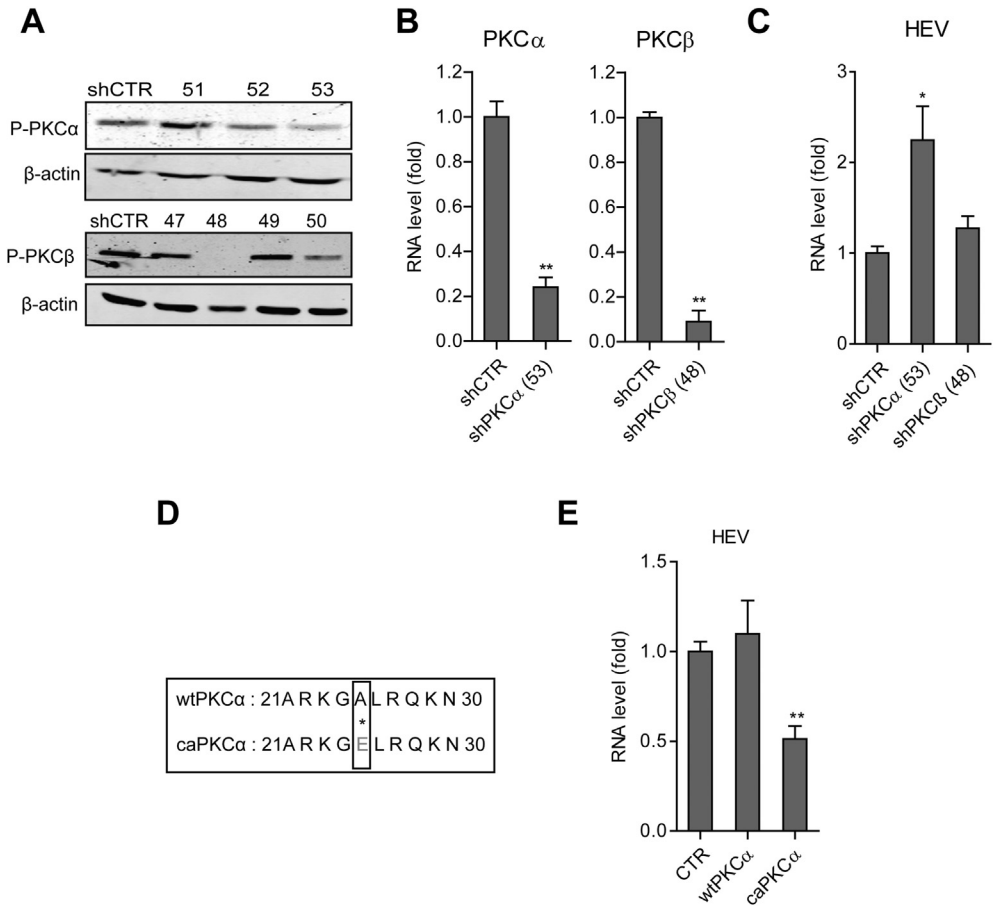

Fig. 2. PKCα is the key antiviral isoform against HEV. (A) Western blot analysis of PKCα and PKCβ knockdown by lentiviral shRNA vectors. Compared with the control vector transduced cells, the shPKCα clone 53 and shPKCβ clone 48 exert potent silencing capability shown at protein levels. Blots depict phosphorylated PKCα, PKCβ and β-actin. (B) qRT-PCR analysis of PKCα and PKCβ knockdown by lentiviral shRNA vectors. Compared to the control vector transduced cells, the no.53 and 48 clones of shPKCα and PKCβ, respectively, exert a potent silencing capability shown at RNA levels (n = 3). (C) Cellular HEV RNA level in PKCα or PKCβ knockdown cells was determined by qRT-PCR 48 h post-inoculation with HEV particles. Knockdown of PKCα led to a 2.25 ± 0.3 fold increase of HEV RNA; whereas PKCβ knockdown resulted in no significant increase (n = 4). (D) The change in amino acid sequence between wtPKCα and caPKCα is shown in the rectangular frame. (E) qRT-PCR analysis of cellular HEV RNA level in CTR, wtPKCα or caPKCα over-expressing cells after inoculation of infectious HEV particles for 72 h caPKCα over-expression inhibited HEV RNA by 49%. Data presented as mean ± SEM (*, $P < 0.05$; **, $P < 0.01$; ***, $P < 0.001$; ns, not significant).

*aattc*AGTCACGTCTTCCCTTTCAGTCACGTCTTCCCTTTCAGTCACGTCT-TCCCTTTCAGTCACGTCTTCCCTTT*a*-3′; Reverse: 5′-*ctagt*AAAGGGA-AGACGTGACTGAAAGGGAAGACGTGACTGAAAGGGAAGACGTGACT-GAAAGGGAAGACGTGACT*g*-3′), which shows no consensus sequence with AP-1 motif. EcoRI and SpeI sites are included (shown in italics) to facilitate directional cloning into the pGreenFire Lenti-Reporter vector (System Biosciences). The recombinant plasmid was verified by restriction enzyme digestion and DNA sequencing. Stable mutant ISRE reporter cells were generated after the lentiviral vector transduction and puromycin (2.5 μg/ml; Sigma) selection.

2.11. C-Fos ChIP-seq data analysis

The c-Fos ChIP-seq data set with accession number GSM754332 was retrieved from the Gene Expression Omnibus. Sequence reads with low complexity that are unlikely to map uniquely to the genome were removed from the dataset using prinseq-lite with the dust method with 7 as threshold (Schmieder and Edwards, 2011; Wang et al., 2016b). Bases on 5′ and 3′ end of the reads with a quality score below 28 were trimmed also using prinseq-lite. Trimmed reads were required to have a minimum length of 20 bases. The remaining sequences with a Phred score <70 were mapped to the hg38 reference genome using Bowtie v0.12.7 (Langmead and Jha, 2009), where we used a seed length of 36 in which we allowed a maximum of 2 mismatches. If a read had multiple alignments, only the best matching read was reported. Duplicated reads were removed. MACS v1.4.2 was used for peak calling using default settings. The sequencing profiles of c-Fos were created in the IGV browser (Robinson et al., 2011).

2.12. MTT assay

Cells were seeded in 96-well plates and cultured at 37 °C with 5% CO_2 for 24, 48, 72 h, respectively. Then 10 mM 3-(4,5-dimethylthiazol-2-yl)-2,5-diphenyltetrazolium bromide (MTT) (Sigma) was added to cells and incubated for 4 h. Subsequently, medium was removed and 100 μl of DMSO was added to each well. The absorbance of each well was read on a microplate absorbance readers (BIO-RAD) at a wavelength of 490 nm. All measurements were performed in triplicate.

2.13. Statistical analysis

All results were presented as mean ± SEM. Comparisons between groups were performed with Mann-Whitney test. Differences were considered significant at a P value less than 0.05.

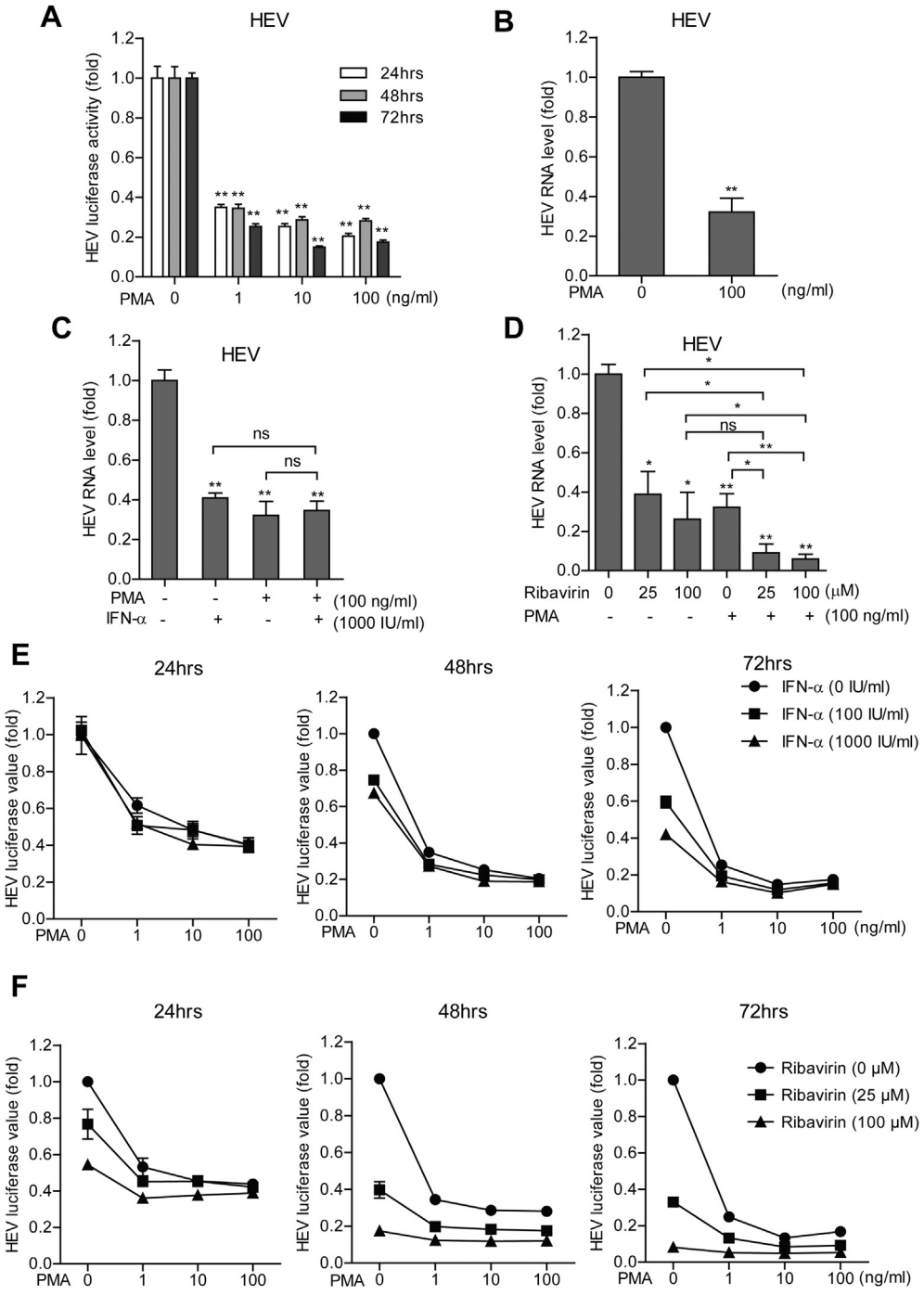

Fig. 3. PKC specific activator PMA exerts strong antiviral activity against HEV. (A) In the Huh7 cell-based subgenomic HEV replicon model, treatment with different doses of PMA inhibited HEV replication-related luciferase activity (n = 3 independent experiments with2−3 replicates each). (B) qRT-PCR analysis of HEV RNA derived from Huh7 cells harboring the full-length HEV infectious genome. Treatment with PMA (100 ng/ml) for 48 h significantly inhibited cellular HEV RNA by 68% (n = 9). (C) Huh7 cells harboring the full-length HEV infectious genome were treated with different doses of IFN-α, PMA or a combination of both for 48 h. Cellular HEV RNA level was determined by qRT-PCR. PMA and IFN-α showed comparable anti-HEV capacity, but they failed to exert further combined effect (n = 4). (D) Same as (C) for ribavirin, PMA or a combination of both. The combination of PMA with ribavirin showed strong additive anti-HEV effect (n = 4). (E) The Huh7 cell-based subgenomic HEV replicon was treated with PMA, IFN-α or a combination of both. Their combination showed no additive effect. Luciferase values were measured at 24, 48 and 72 h (n = 3 independent experiments with 2−3 replicates each). (F) Same as (E) for PMA, ribavirin or a combination of both. Their combination showed additive anti-HEV activity. (n = 3 independent experiments with 2−3 replicates each). Data presented as mean ± SEM (*, *P < 0.05*; **, *P < 0.01*; ***, *P < 0.001;* ns, not significant).

3. Results

3.1. A screening for kinases identifies conventional PKCs as cell-autonomous anti-HEV elements

Protein kinases are pivotal mediators of signal transduction and identifying kinases involved in biological responses can shed important light on kinase associated virus-host interactions. The lack of understanding as to which signal pathways mediate cell-autonomous antiviral immunity against HEV thus prompted us to execute a screening of kinase inhibitors with respect to their effects in antiviral responses. To this end, we employed a hepatocyte cell

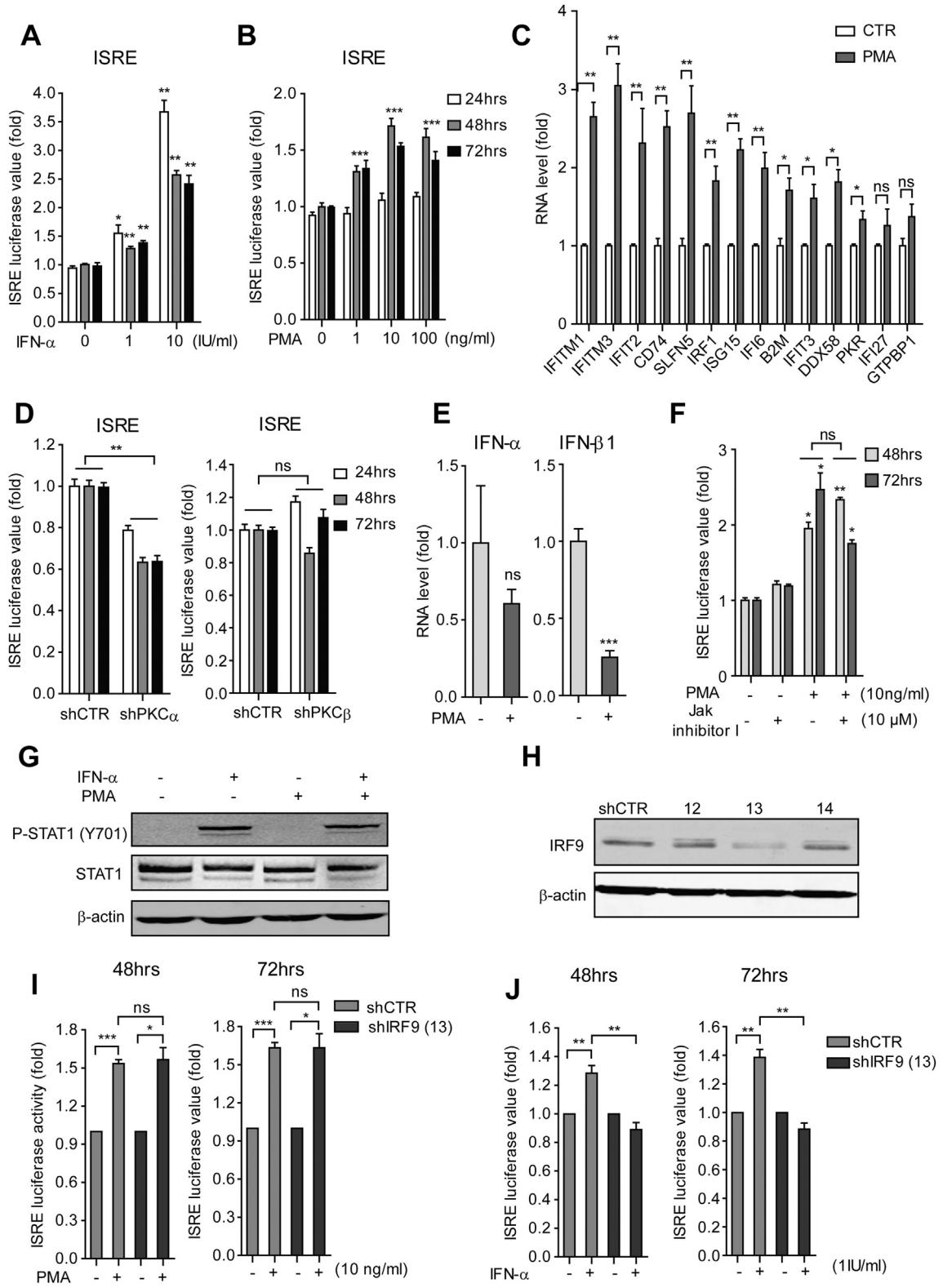

Fig. 4. PKCα provokes transcriptional activation of ISGs, independent of IFN-JAK-STAT pathway. (A) In Huh7 based ISRE luciferase reporter cells, treatment with IFN-α resulted in a dose-dependent induction of ISRE-related luciferase activity (n = 3 independent experiments with 2–3 replicates each). (B) Same as (A) for PMA. (C) After PMA (100 ng/ml) treatment, expression profile of 14 different ISGs in Huh7 cells was quantified by qRT-PCR. Except for IFI27 and GTBP1, other ISGs were significantly induced (n = 6). (D) Knockdown PKCα by lentiviral shRNA vector (No. 48) in Huh7 based ISRE luciferase reporter cells resulted in significant inhibition of ISRE-related luciferase activity; while PKCβ knockdown (No. 53) had no significant effect (n = 3 independent experiments with 2–3 replicates each). (E) qRT-PCR analysis of IFN-α and β1 expression levels in Huh7 cells treated with PMA (100 ng/ml) (n = 3). (F) ISRE luciferase activity was measured, after treatment with JAK inhibitor I, PMA or a combination of both for 48 and 72 h (n = 3 independent experiments with 2–3 replicates each). (G) Phosphorylated STAT1 protein level was detected by western blot, after treatment with IFN-α (1000 IU/ml), PMA (100 ng/ml) or a combination of both. (H) Western blot analysis of IRF9 knockdown by lentiviral shRNA vectors in the Huh7 based ISRE luciferase reporter cells. Compared to the control vector transduced cells, the clone NO.13 of shIRF9 exerts strong silencing capability shown at protein levels. Blots depict IRF9 and β-actin. (I) Knockdown of IRF9 in Huh7 based ISRE luciferase reporter cells has

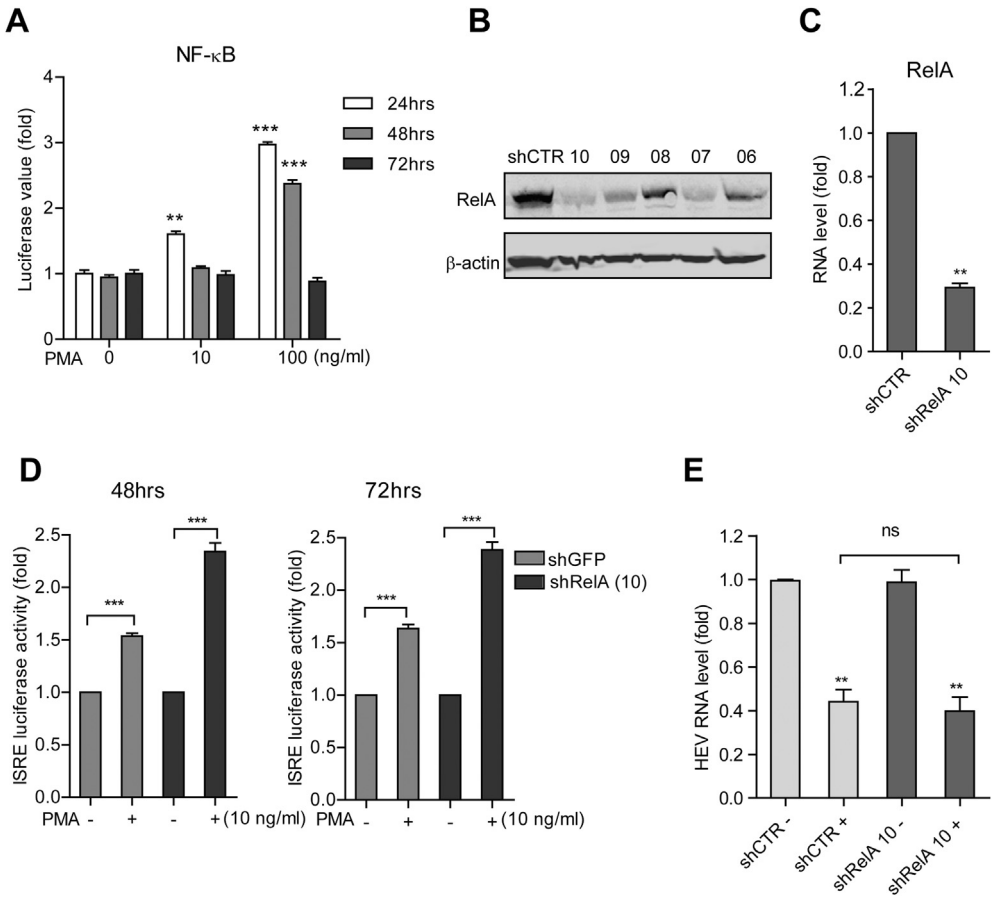

Fig. 5. PKCα mediated anti-HEV activity is independent of NF-κB signaling. (A) In Huh7 based NF-κB luciferase reporter cells, treatment with PMA resulted in a dose-dependent induction of NF-κB related luciferase activity (n = 3 independent experiments with 2–3 replicates each). (B) Western blot analysis of RelA knockdown by lentiviral shRNA vectors in Huh7 cells. Blots depict RelA and β-actin. (C) qRT-PCR analysis of RelA knockdown by lentiviral shRNA vectors at RNA level (n = 3). (D) Knockdown of RelA in Huh7 based ISRE luciferase reporter cells did not block PMA induced ISRE-related luciferase activation measured at 48 and 72 h (n = 3 independent experiments with 2–3 replicates each). (E) Knockdown of RelA did not block PMA induced anti-HEV activity as determined by qRT-PCR 48 h post-inoculation with HEV particles (n = 4). Data presented as mean ± SEM (*, *P < 0.05*; **, *P < 0.01*; ***, *P < 0.001;* ns, not significant).

line, i.e. Huh7, transfected with a HEV replicon luciferase reporter as a platform for the screening of 132 pharmacological kinase inhibitors with known specificity profile (Debing et al., 2014) (Fig. S1A and Table S1). We arbitrarily set the control luciferase value to 1 and identified 40 inhibitors (normalized value $\geq$ 1.2) that increase and 42 compounds (normalized value $\leq$ 0.8) that inhibit luciferase activity in this assay system (Fig. 1A and Table S2). Inhibition of luciferase activity might be due to non-specific effects not related to the scientific question at hand (*e.g.* effects on translation or cell survival). Strikingly, stimulation of luciferase activity likely relates to the inhibition of signaling elements involved in constraining viral replication and hence we concentrated on luciferase enhancing compounds in our search for elements involved in antiviral immunity. Go6976, a fairly specific inhibitor of the conventional PKCs (PKCα, $PKC\beta_I$, $PKC\beta_{II}$, and PKCγ) (Martiny-Baron et al., 1993), has increased HEV luciferase activity. Subsequent western blot analysis for the phosphorylation state of PKC isoforms confirmed the inhibition of PKCα and PKCβ by Go6976 in our experimental system (Fig. 1B). HEV promoting activity of Go6976 was further confirm in two independent cell culture models: a subgenomic HEV containing luciferase reporter and a full-length HEV infectious cell culture system (Fig. 1C, D and Fig. S1B). Go6976 showed inhibitory effect on host cell growth (Fig. S1C), which is expected because of the crucial roles of PKCs in cell physiology. Interestingly, Go6976 is also indicated as a potential inhibitor of protein kinase D (PKD), although with relatively lower sensitivity compared with PKCα and PKCβ1. Therefore, we also tested the role of PKD in Go6976 induced HEV replication. CID 755673, a selective PKD inhibitor (IC_{50}: 0.182–0.227 μM) was tested in both HEV cell culture systems. However, CID 755673 showed no significant effect on HEV replication (Fig. S1D and E). Therefore, the effect of Go6976 on HEV is likely independent of PKD. Collectively, these data demonstrated that conventional PKCs are important antiviral elements, at least with respect to HEV infection.

3.2. PKCα is the key anti-HEV isoform

The observation that conventional PKCs constrain HEV replication raises questions as to the role of different PKC isoforms. To dissect the effects of individual PKC isoforms, we silenced the

no effect on PMA induced ISRE-related luciferase activation, as measured at 48 and 72 h (n = 3 independent experiments with 2–3 replicates each). (J) Knockdown of IRF9 in the Huh7 based ISRE luciferase reporter cells blocks IFN-α (1 IU/ml) induced ISRE-related luciferase activation, as measured at 48 and 72 h (n = 3 independent experiments with 2–3 replicates each). Date presented as mean ± SD (*, *P < 0.05*; **, *P < 0.01*; ***, *P < 0.001;* ns, not significant).

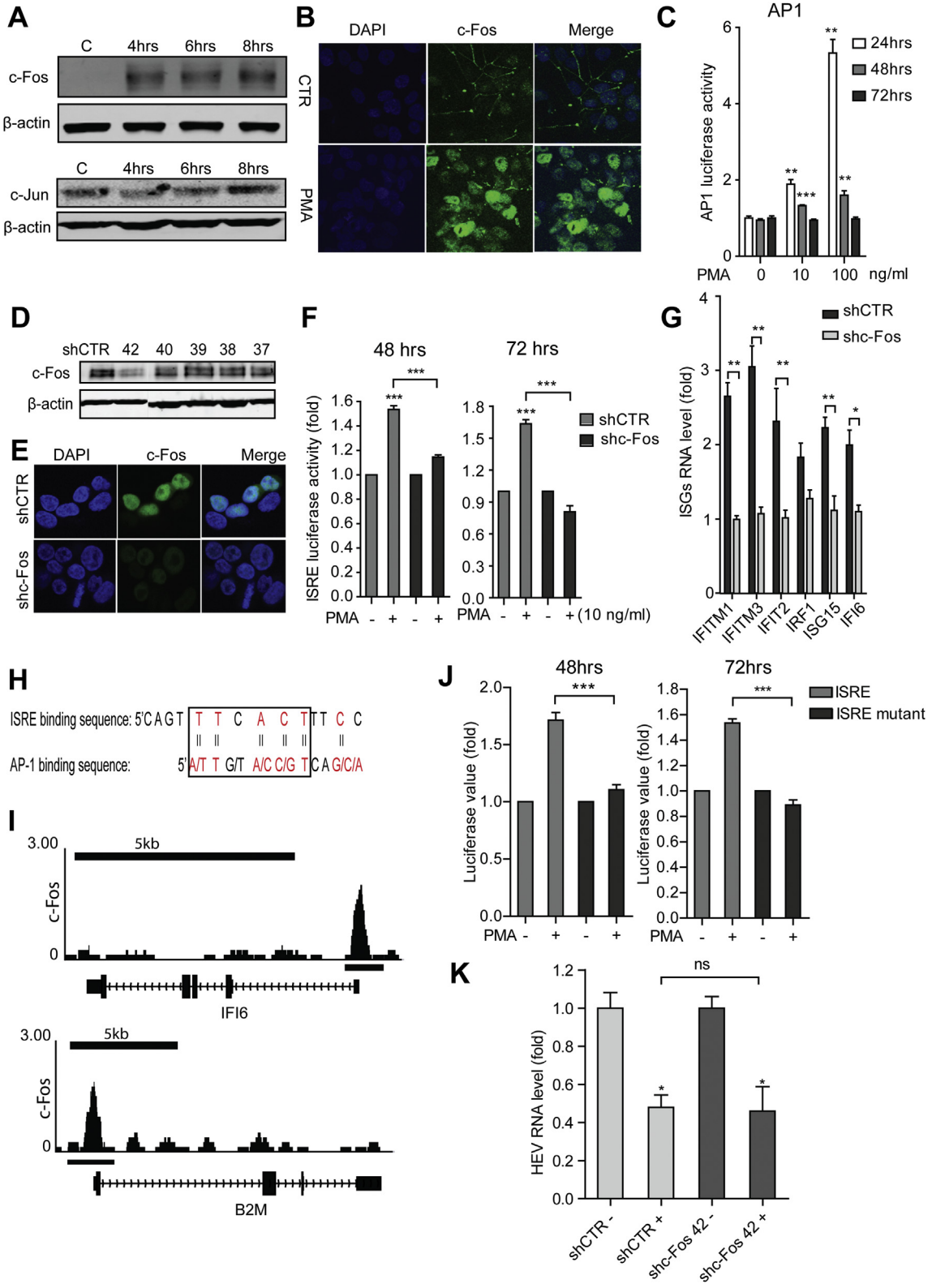

Fig. 6. PKCα/AP1 serves as a non-canonical mechanism to mediate ISG transcription, but is not essential for PKCα-mediated anti-HEV activity. (A) Western blot analysis of c-Fos and c-Jun protein levels in Huh7 cells treated with PMA (100 ng/ml) for 4, 6 and 8 h. PMA stimulation provokes strong induction of c-Fos. (B) Confocal microscopy analysis of c-Fos localization in Huh7 cells treated with PMA for 4 h c-Fos was induced and translocated to nucleus upon PMA stimulation. c-Fos antibody (green). Nuclei were visualized by DAPI (blue). (C) In Huh7 based AP-1 luciferase reporter cells, treatment with PMA resulted in dose-dependent induction of AP-1-related luciferase activity (n = 3 independent experiments with 2–3 replicates each). (D) Western blot analysis of c-Fos knockdown by lentiviral shRNA vectors. Compared to the control vector transduced cells, the NO.42 clone of shc-Fos exerts potent silencing capability shown at protein levels. Blots depict c-Fos and β-actin. (E) Confocal microscopy analysis confirmed profound down-regulation of c-Fos after knockdown by lentiviral shRNA vectors. C-Fos antibody (green). Nuclei were visualized by DAPI (blue). (F) Knockdown of c-Fos in Huh7 based ISRE luciferase reporter cells demolished PMA induced ISRE-related luciferase activation, as measured at 48 and 72 h (n = 3 independent experiments with 2–3 replicates each). (G) qRT-PCR analysis confirmed

expression of *PRKCA* (the gene coding for PKCα) and *PRKCB* (that gives rise to $PKC\beta_I$ and $PKC\beta_{II}$) in Huh7 cells using lentiviral-mediated RNAi. Since PKCγ has been shown to be specifically expressed in neuronal tissue (Martiny-Baron and Fabbro, 2007), we ruled it out for further research. Western blot and qRT-PCR confirmed successful down-regulation of PKC isoforms (Fig. 2A and B) at protein and RNA levels. Subsequently, cells were inoculated with infectious HEV particles and cellular HEV RNA was quantified by qRT-PCR after 48 h. Knockdown of PKCα led to a 2.25 ± 0.3 fold ($n = 4$, $p < 0.05$) increase of HEV RNA; whereas PKCβ knockdown resulted in no significant effect (Fig. 2C), suggesting that PKCα is the relevant isoform here.

PKCα maintains its inactive state via an inhibitory region within the effector binding domain of the kinase. Its pseudosubstrate site mediates this inhibition by binding to the active site and preventing substrate interaction (House and Kemp, 1987). A constitutively active PKCα (caPKCα) is available in which a glutamic acid present in this region is substituted for alanine. (Fig. 2D). This form dramatically increases effector-independent kinase activity, compared to the wild-type PKCα (wtPKCα) (Pears et al., 1990). Huh7 cells were transduced with integrating lentiviral vectors co-expressing GFP and caPKCα or wtPKCα (Fig. S1F). Cell cytometry confirmed transgene expression by measuring GFP and positive cells were sorted and expanded for further experimentation (Fig. S1G). Huh7 cells expressing caPKCα or wtPKCα were inoculated with infectious HEV particles and relative viral RNA level was quantified 48 h post-inoculation. Consistent with PKCα knockdown (Fig. 2C), expression of caPKCα significantly decreased HEV RNA by 49% ($n = 4$, $p < 0.05$), while wtPKCα over-expression showed no effect on HEV compared to control sample (Fig. 2E).

This promising result prompted us to investigate the potential role of the classical PKC pharmacological activator, PMA, also commonly known as 12-*O*-Tetradecanoylphorbol-13-acetate (TPA). PMA, structurally analogous to diacylglycerol, is commonly used to activate PKC. It is also a promising drug candidate, currently under a Phase II clinical trial for the treatment of patients with relapsed/refractory acute myelogenous leukemia (NCT01009931). As expected, PMA exerted strong anti-HEV effects in both HEV subgenomic and full-length infectious models (Fig. 3A and B and Fig. S2A, B); while no clear effect on cell growth and viability was observed (Fig. S2C). This result prompted us to assess the combined antiviral effect of PMA with the off-label anti-HEV drugs IFN-α or ribavirin (Debing et al., 2014; Todt et al., 2016; Zhou et al., 2016). Although PMA and IFN-α showed comparable anti-HEV capacity, they failed to exert further combined effect (Fig. 3C and E). The combination of PMA with ribavirin showed strong additive anti-HEV effect (Fig. 3D and F). These data collectively indicate that activated PKCα plays an important role in cell-autonomous anti-HEV immunity.

3.3. PKCα provokes transcriptional activation of ISGs, independent of the IFN-JAK-STAT pathway

We extended our study on a list of other viruses (rotavirus, murine norovirus, HIV-1 and influenza virus). Although no significant antiviral effects on HIV-1 and influenza virus, PMA significantly inhibited rotavirus and murine norovirus 1 infection (Fig. S2B - G). The relative broad antiviral efficacy induced by PMA prompted us to investigate its potential link to the function of IFNs, which possess broad antiviral effects via efficient induction of ISGs.

Following interferon stimulation and interferon receptor activation, STAT1 and STAT2 are phosphorylated and form heterodimers, which subsequently bind to IRF9 leading to the formation of the so-called IFN-stimulated gene factor 3 (ISGF3) complex. ISGF3 translocates to the nucleus and binds to the DNA specific sequence motif [5′-CAGTTTCACTTTCC-3′], ISREs, to drive the expression of ISGs, which are the ultimate antiviral effectors of the interferon cascade (Fig. 4A) (Ohmori and Hamilton, 1993). As expected, employing a Huh7 stably transfected ISRE-driven luciferase reporter cell line (Pan et al., 2011), we observed the induction of luciferase activity with IFN-α stimulation (Fig. 4A). Surprisingly, forced activation of PKC, using the PMA stimulus, also provokes transactivation of ISRE elements (Fig. 4B). Further confirmation was obtained by quantification of a panel of well-known antiviral ISGs (Fig. 4C). Importantly, when the ISRE reporter cell line was transduced with integrating lentiviral vectors expressing shRNA specifically targeting PKCα, β or a control shRNA (shCTR), PKCα silencing resulted in a significant decrease of ISRE luciferase activity compared with shCTR control; whereas PKCβ knockdown did not significantly affect ISRE activity (Fig. 4D). These data demonstrate that PMA activates PKCα to mediate the transcriptional activity of ISRE, resulting in the induction of antiviral ISGs.

Signal transduction of the IFN-α/β receptor appears kaleidoscopic in that multiple discrete signaling cassettes are activated. An important effector is phosphatidylinositol-3OH-kinase (PI3) kinase, a major regulator of cellular signaling. Activation of PI3 kinase in turn leads to the activation of various effector pathways in different cell types, including 3-phosphoinositide dependent protein kinase (PDK), Protein kinase B (PKB), mechanistic target of rapamycin (mTOR) and PKC (Fig. S3B) (Kaur et al., 2005). As PI3 kinase signaling and other signaling cassettes downstream of the interferon receptors may (in)directly crosstalk with PKCα, we investigated possible effects of IFN-α on PKC activation. As determined by western blot, PKC α/β are not activated upon IFN-α challenge (1000 IU/ml; Fig. S3C). Thus, PKCα activation is not the downstream effect of the IFN receptor.

To further investigate whether PKCα activation results in direct ISRE activation or whether indirect autocrine/paracrine mechanisms are responsible, we investigated possible PMA effects on the expression of type I interferons. PMA treatment did not increase IFN-α mRNA but even slightly decreased IFN-β1 expression (Fig. 4E). In apparent agreement, incubation with the *pan*-JAK inhibitor I abrogated STAT1 phosphorylation and the induction of ISRE-regulated luciferase activity in Huh7 cells even following high dose IFN-α treatment (1000 IU/ml) (Fig. S3D and E), but did not diminish PMA-induced ISRE activation (Fig. 4F). Furthermore, PMA did not affect STAT1 phosphorylation or IFN-α induced STAT1 activation at amino acid 701 (Y701P), which is an indispensable signature of STAT1 activation (Fig. 4G). We further examined the role of IRF9, a key downstream element antiviral effector of the interferon pathway. As expected, PMA-induced ISRE luciferase activity was not affected in IRF9 knockdown cells compared to the shCTR control (Fig. 4H and I); whereas IFN-α induced activation was

that the induction of ISGs by PMA was largely abrogated after c-Fos knockdown ($n = 3$). (H) ISRE and AP-1 sequence specific binding regions. Their consensus nucleotides are labeled in red color, and the consensus region is enclosed by the rectangular box. (I) Examples of two ISG genes with c-Fos binding to their promoter regions. The normalized binding signals were used as the input data. Binding peak detection was performed with PeakSeq v1.01 for identifying and ranking peak regions in ChIP-Seq data analysis. The Y axis value represents the binding signaling value; the black bar in the right corner represent the scale (5k bp). (J) Huh7 cells carrying the ISRE mutated luciferase reporter showed demolished activation upon PMA stimulation, as measured at 48 and 72 h ($n = 3$ independent experiments with 2–3 replicates each). (K) Knockdown of c-Fos in Huh7 cells did not abrogate PMA induced anti-HEV activity as determined by qRT-PCR 48 h post inoculation with HEV particles ($n = 4$). Data presented as mean ± SEM (*, $P < 0.05$; **, $P < 0.01$; ***, $P < 0.001$; ns, not significant). (For interpretation of the references to colour in this figure legend, the reader is referred to the web version of this article.)

clearly impaired (Fig. 4J and Fig. S3F). These results collectively indicate that PKCα-induced ISRE activation is independent of the classical interferon pathway.

3.4. PKCα mediated ISG transcriptional activation and anti-HEV effect is independent of the NF-κB pathway

NF-κB signaling is a central pathway involved in cellular innate immune response. PMA can activate NF-κB signaling via the phosphorylation of NF-κB/p65 by PKCα (Chang et al., 2005; Jiang et al., 2010; Mut et al., 2010). Thus, we investigated the potential involvement of NF-κB pathway. To this end, we used a lentiviral transcriptional reporter system expressing the firefly luciferase gene under the control of NF-κB responsive promoter. Huh7 cells were transduced with the vector to create a stable NF-κB reporter cell line. As expected, stimulation with PMA led to the strong activation of NF-κB luciferase activity (Fig. 5A) and thus a role of NF-κB signaling cannot be ruled out. Thus, the Huh7 cell line was transduced with integrating lentiviral shRNA vectors to silence RelA (P65), an essential subunit of the NF-κB transcription complex, resulting in profound down-regulation of RelA expression (Fig. 5B and C). These cells, however, still showed ISRE-driven luciferase activation (Fig. 5D). Consistently, PMA induced anti-HEV effect was not abrogated in RelA knockdown cells (Fig. 5E). Thus, NF-κB signaling appears not to be involved in PKCα mediated ISG transcriptional activation and anti-HEV effect.

3.5. PKCα/AP1 represents a non-canonical mechanism of activating ISG transcription, but is dispensable for PKCα-mediated anti-HEV activity

AP-1 signaling is another important pathway involved in cellular innate immune response. PMA can also activate AP1 signaling via the activation of PKCα (Hwang et al., 2010; Langlet et al., 2010). Indeed, PMA stimulation provokes a strong induction of c-Fos, an essential subunit of the AP1 transcription complex (Fig. 6A). Accordingly, unstimulated cells displayed hardly detectable c-Fos protein, but c-Fos was substantially induced and translocated to nucleus following PMA stimulation (Fig. 6B). Convincingly, we also used a lentiviral transcriptional reporter system expressing the firefly luciferase gene under control of an AP-1 responsive promoter. Huh7 cells were transduced with the vector to create a stable AP-1 reporter cell line. As shown in Fig. 6C, stimulation with PMA led to the strong activation of AP-1 luciferase activity. Thus, to determine the role of AP-1 activation, Huh7 cells were transduced with integrating lentiviral RNAi vectors to silence *c*-Fos (Fig. 6D and E). Surprisingly, PMA induced ISRE activation was abrogated in c-Fos knockdown cells (Fig. 6F). Consistently, the induction of ISGs by PMA was also sensitive to c-Fos knockdown (Fig. 6G). Thus, AP-1 appears essential for PKCα-mediated ISRE activation.

Upon signaling activation, the transcription factor, AP-1, can bind to the sequence specific palindromic AP-1 site [5'-(A/T)T(G/T)(A/C)(G/C)TCA(G/C/A)-3'] to promote gene transcription (Colin et al., 2011; Hess et al., 2004). The puzzling role of AP-1 in the transactivation of the ISRE led us to perform an *in silico* analysis comparing the ISRE motif and the AP-1 DNA binding site and surprisingly revealed a consensus sequence of these two motifs (Fig. 6H). We thus hypothesized that AP-1 might bind to this consensus sequence within the ISRE motif to drive its transcription. To test this hypothesis, we retrieved genome wide c-Fos ChIP-Seq data from GEO database (GSM754332) and analyzed the data set using Integrative Genomics Viewer (IGV) (Fig. S4A) (Consortium, 2012; Robinson et al., 2011; Thorvaldsdottir et al., 2013). Confirming our hypothesis, we found c-Fos binding to the promoter regions of a list of ISGs (Fig. S5). To further confirm this notion, we mutated the consensus nucleotide sequence within the ISRE motif based on the lentiviral transcriptional reporter vector expressing the firefly luciferase gene driven by multiple ISREs, resulting in a mutant ISRE luciferase reporter vector that should not be capable of AP-1 binding. (Fig. S4B). Huh7 cells were transduced with this vector to create a stable reporter cell line. As expected, PMA failed to activate this mutated ISRE (Fig. 6J). Hence, AP-1 is capable of direct transactivation of the ISRE. Surprisingly, PMA mediated anti-HEV activity was not abrogated in c-Fos knockdown cells (Fig. 5K), even though the ISRE activation and ISG induction was blocked. Thus, AP-1 mediated ISG induction appears not essential for PKCα-mediated anti-HEV activity.

4. Discussion

Protein kinases play pivotal roles in regulating immune responses either positively or negatively via regulating protein functions, signal transduction or other cellular processes(Georgel et al., 2010; Li et al., 2014; Lupberger et al., 2013). This study comprehensively profiled kinase-mediated cascades in cell–autonomous antiviral immunity via screening a library of pharmacological kinase inhibitors on Huh7 based HEV replication cell model. We identified PKCα as an important antiviral host factor and a targetable host factor for antiviral drug development. Both functional over-expression and pharmacological activation showed strong and comparable anti-HEV activity compared to IFN-α.

PMA, as a phorbol ester, binds to the C1 domain in the regulatory region of PKCs to promote their activation (Ono et al., 1989). Although PMA was reported to have a potential tumor-promoting role in experimental skin cancer mouse models (Furstenberger et al., 1981), its anti-cancer activity in fact has been extensively investigated in the clinic, including in patients with hematological malignancy, squamous cell carcinoma, renal cell carcinoma, ovarian teratocarcinoma, subcutaneous adenocarcinoma and prostate cancer (Schaar et al., 2006). Cancer patients often suffer from depressed white blood cell and neutrophil counts because of chemotherapeutic drugs. PMA treatment has been shown to increase white blood cell and neutrophil counts towards a normal range with only mild and reversible side effects observed (Han et al., 1998). A Phase I trial of treating hematologic cancer or bone marrow disorder with PMA has been successfully conducted at The State University of New Jersey (NCT00004058). The same institute is currently pursuing a Phase II trial plus dexamethasone & choline magnesium trisalicylate in the treatment of patients with relapsed/refractory acute myelogenous leukemia (NCT01009931). An interesting link is that patients with leukemia or other cancers are prone to virus infections, including HEV (Geng et al., 2014; Motte et al., 2012; Pfefferle et al., 2012). The potential clinical prospects of PMA or its derivatives may be of achieving “one stone two birds” effects: simultaneously combating cancer and virus.

An interesting point of this study is the discovery of a new mechanism in transcription of antiviral ISGs, although moderately. Classically, ISG induction was known to be initiated predominantly by the IFN-JAK-STAT pathway in cell-autonomous defense against viral infection. Upon phosphorylation, STAT1 and STAT2 forming a complex with IRF9, this ISGF3 complex translocates to the nucleus and binds to the ISRE to drive ISG transcription. Here, we demonstrated that activation of the PKCα/AP-1 cascade was able to moderately drive ISG transcription as well. This action is independent of IFN production and the canonical JAK-STAT machinery. AP-1 is a transcription complex mainly composed of c-Jun and c-Fos proteins forming a heterodimers through their leucine-zipper domains. The AP-1 dimers recognize the sequence specific response elements via the basic domain and regulate target genes involved in

cell proliferation, differentiation and apoptosis (Zenz et al., 2008). Surprisingly, we observed consensus sequence between the ISRE and the AP-1 DNA binding site. Using ChIP-Seq data analysis and loss-of-function mutagenesis assays, we firmly demonstrated that AP-1 could directly drive gene transcription through binding to the ISRE on the ISG promoter region. Of note, the ISG induction effect induced by the PKCα/AP1 pathway is moderate, this may explain its non-essential role for PKCα-mediated anti-HEV activity.

In conclusion, we identified PKCα as an important cell-autonomous antiviral factor against HEV in host defense. In addition, we also revealed a non-canonical mechanism in transcriptional activation of ISGs, although this is dispensable for PKCα-mediated antiviral activity. These results provide valuable antiviral target and shed new insights of virus-host interactions.

Author contributions

W.W. contributed to study concept and design; acquisition of data; analysis and interpretation of data; drafting of the manuscript; statistical analysis; Y. W., X. Z., Y.Y. and L.X. contributed to acquisition of data and critical revision of the manuscript; E. H. C. and B. B. carried out HIV-1 experiments and critical revision of the manuscript; J. B. and R. P. were involved in ChIP-Seq database analysis; Y. D. and J. N. helped with kinase inhibitor library screening and critical revision of the manuscript; M. P. P. contributed to study concept, study supervision and critical revision of the manuscript; Q. P. contributed to study concept and design, obtained funding, study supervision and critical revision of the manuscript.

Conflict of interest statement

The authors have declared that no conflict of interest exists.

Acknowledgements

The authors gratefully thank Dr. Patrick Chaltin and Arnaud Marchand for the availability of the cell kinase inhibitors; Dr. Suzanne U. Emerson (National Institute of Allergy and Infectious Diseases, NIH, USA) for generously providing the plasmids to generate subgenomic and full-length HEV genomic RNA; Dr. Herbert W. Virgin (Washington University School of Medicine, USA) for providing the mouse norovirus strain; Dr. Hong-Yiou Lin (University of Minnesota) providing the over-expression PKCα lentiviral vector. Dr. Miranda de Graaf (Department of Viroscience, Erasmus Medical Center, Netherlands) for the help with influenza replication curves. The authors also would like to acknowledge the ENCODE Consortium and the ENCODE production laboratory(s) generating the c-Fos ChIP-Seq dataset (GSM754332). This research is supported by the Netherlands Organisation for Scientific Research for a VENI grant (No. 916-13-032 to Q. P.), the Dutch Digestive Foundation for a career development grant (No. CDG 1304 to Q. P.), the Daniel den Hoed Foundation for a Centennial Award fellowship (to Q. P.), European Association for the Study of the Liver (EASL) for a Sheila Sherlock Fellowship (to Q. P.) and the China Scholarship Council for funding PhD fellowships (201303250056 to W. W.), (201207720007 to Y. W.), (201206150075 to X. Z.), (201307720045 to Y. Y.) and (201306300027 to L. X.). Y. Debing is a fellow of the Research Foundation − Flanders (FWO).

Appendix A. Supplementary data

Supplementary data related to this article can be found at http://dx.doi.org/10.1016/j.antiviral.2017.01.005.

References

Chang, M.S., Chen, B.C., Yu, M.T., Sheu, J.R., Chen, T.F., Lin, C.H., 2005. Phorbol 12-myristate 13-acetate upregulates cyclooxygenase-2 expression in human pulmonary epithelial cells via Ras, Raf-1, ERK, and NF-kappa B, but not p38 MAPK, pathways. Cell. Signal. 17, 299–310.

Colin, L., Vandenhoudt, N., de Walque, S., Van Driessche, B., Bergamaschi, A., Martinelli, V., Cherrier, T., Vanhulle, C., Guiguen, A., David, A., Burny, A., Herbein, G., Pancino, G., Rohr, O., Van Lint, C., 2011. The AP-1 binding sites located in the pol gene intragenic regulatory region of HIV-1 are important for viral replication. PLoS One 6, e19084.

Consortium, E.P., 2012. An integrated encyclopedia of DNA elements in the human genome. Nature 489, 57–74.

de Wilde, A.H., Jochmans, D., Posthuma, C.C., Zevenhoven-Dobbe, J.C., van Nieuwkoop, S., Bestebroer, T.M., van den Hoogen, B.G., Neyts, J., Snijder, E.J., 2014. Screening of an FDA-approved compound library identifies four small-molecule inhibitors of Middle East respiratory syndrome coronavirus replication in cell culture. Antimicrob. Agents Chemother. 58, 4875–4884.

Debing, Y., Emerson, S.U., Wang, Y., Pan, Q., Balzarini, J., Dallmeier, K., Neyts, J., 2014. Ribavirin inhibits in vitro hepatitis E virus replication through depletion of cellular GTP pools and is moderately synergistic with alpha interferon. Antimicrob. Agents Chemother. 58, 267–273.

Furstenberger, G., Berry, D.L., Sorg, B., Marks, F., 1981. Skin tumor promotion by phorbol esters is a two-stage process. Proc. Natl. Acad. Sci. U. S. A. 78, 7722–7726.

Geng, Y., Zhang, H., Huang, W., T, J.H., Geng, K., Li, Z., Wang, Y., 2014. Persistent hepatitis e virus genotype 4 infection in a child with acute lymphoblastic leukemia. Hepat. Mon. 14, e15618.

Georgel, P., Schuster, C., Zeisel, M.B., Stoll-Keller, F., Berg, T., Bahram, S., Baumert, T.F., 2010. Virus-host interactions in hepatitis C virus infection: implications for molecular pathogenesis and antiviral strategies. Trends Mol. Med. 16, 277–286.

Hakim, M.S., Wang, W., Bramer, W.M., Geng, J., Huang, F., de Man, R.A., Peppelenbosch, M.P., Pan, Q., 2017 Jan. The global burden of hepatitis E outbreaks: a systematic review. Liver Int. 37 (1), 19–31.

Han, Z.T., Tong, Y.K., He, L.M., Zhang, Y., Sun, J.Z., Wang, T.Y., Zhang, H., Cui, Y.L., Newmark, H.L., Conney, A.H., Chang, R.L., 1998. 12-O-Tetradecanoylphorbol-13-acetate (TPA)-induced increase in depressed white blood cell counts in patients treated with cytotoxic cancer chemotherapeutic drugs. Proc. Natl. Acad. Sci. U. S. A. 95, 5362–5365.

Hess, J., Angel, P., Schorpp-Kistner, M., 2004. AP-1 subunits: quarrel and harmony among siblings. J. Cell Sci. 117, 5965–5973.

House, C., Kemp, B.E., 1987. Protein-Kinase-C contains a pseudosubstrate prototype in its regulatory domain. Science 238, 1726–1728.

Hwang, Y.P., Yun, H.J., Kim, H.G., Han, E.H., Lee, G.W., Jeong, H.G., 2010. Suppression of PMA-induced tumor cell invasion by dihydroartemisinin via inhibition of PKCalpha/Raf/MAPKs and NF-kappaB/AP-1-dependent mechanisms. Biochem. Pharmacol. 79, 1714–1726.

Jiang, R., Teng, Y., Huang, Y., Gu, J., Li, M., 2010. Protein kinase C-alpha activation induces NF-kB-dependent VCAM-1 expression in cultured human umbilical vein endothelial cells treated with sera from preeclamptic patients. Gynecol. Obstet. Investig. 69, 101–108.

Kaur, S., Uddin, S., Platanias, L.C., 2005. The PI3' kinase pathway in interferon signaling. J. Interferon Cytokine Res. 25, 780–787.

Langlet, C., Springael, C., Johnson, J., Thomas, S., Flamand, V., Leitges, M., Goldman, M., Aksoy, E., Willems, F., 2010. PKC-alpha controls MYD88-dependent TLR/IL-1R signaling and cytokine production in mouse and human dendritic cells. Eur. J. Immunol. 40, 505–515.

Langmead, C.J., Jha, S.K., 2009. Symbolic approaches for finding control strategies in Boolean Networks. J. Bioinform Comput. Biol. 7, 323–338.

Li, Q., Zhang, Y.Y., Chiu, S., Hu, Z., Lan, K.H., Cha, H., Sodroski, C., Zhang, F., Hsu, C.S., Thomas, E., Liang, T.J., 2014. Integrative functional genomics of hepatitis C virus infection identifies host dependencies in complete viral replication cycle. PLoS Pathog. 10, e1004163.

Llovet, J.M., Ricci, S., Mazzaferro, V., Hilgard, P., Gane, E., Blanc, J.F., de Oliveira, A.C., Santoro, A., Raoul, J.L., Forner, A., Schwartz, M., Porta, C., Zeuzem, S., Bolondi, L., Greten, T.F., Galle, P.R., Seitz, J.F., Borbath, I., Haussinger, D., Giannaris, T., Shan, M., Moscovici, M., Voliotis, D., Bruix, J., Group, S.I.S., 2008. Sorafenib in advanced hepatocellular carcinoma. N. Engl. J. Med. 359, 378–390.

Lupberger, J., Duong, F.H., Fofana, I., Zona, L., Xiao, F., Thumann, C., Durand, S.C., Pessaux, P., Zeisel, M.B., Heim, M.H., Baumert, T.F., 2013. Epidermal growth factor receptor signaling impairs the antiviral activity of interferon-alpha. Hepatology 58, 1225–1235.

Lupberger, J., Zeisel, M.B., Xiao, F., Thumann, C., Fofana, I., Zona, L., Davis, C., Mee, C.J., Turek, M., Gorke, S., Royer, C., Fischer, B., Zahid, M.N., Lavillette, D., Fresquet, J., Cosset, F.L., Rothenberg, S.M., Pietschmann, T., Patel, A.H., Pessaux, P., Doffoel, M., Raffelsberger, W., Poch, O., McKeating, J.A., Brino, L., Baumert, T.F., 2011. EGFR and EphA2 are host factors for hepatitis C virus entry and possible targets for antiviral therapy. Nat. Med. 17, 589–595.

Martiny-Baron, G., Fabbro, D., 2007. Classical PKC isoforms in cancer. Pharmacol. Res. 55, 477–486.

Martiny-Baron, G., Kazanietz, M.G., Mischak, H., Blumberg, P.M., Kochs, G., Hug, H., Marme, D., Schachtele, C., 1993. Selective inhibition of protein kinase C isozymes by the indolocarbazole Go 6976. J. Biol. Chem. 268, 9194–9197.

Motte, A., Roquelaure, B., Galambrun, C., Bernard, F., Zandotti, C., Colson, P., 2012.

Hepatitis E in three immunocompromized children in southeastern France. J. Clin. Virol. 53, 162–166.
Mut, M., Amos, S., Hussaini, I.M., 2010. PKC alpha phosphorylates cytosolic NF-kappaB/p65 and PKC delta delays nuclear translocation of NF-kappaB/p65 in U1242 glioblastoma cells. Turk Neurosurg. 20, 277–285.
Ohmori, Y., Hamilton, T.A., 1993. Cooperative interaction between interferon (IFN) stimulus response element and kappa B sequence motifs controls IFN gamma- and lipopolysaccharide-stimulated transcription from the murine IP-10 promoter. J. Biol. Chem. 268, 6677–6688.
Ono, Y., Fujii, T., Igarashi, K., Kuno, T., Tanaka, C., Kikkawa, U., Nishizuka, Y., 1989. Phorbol ester binding to protein kinase C requires a cysteine-rich zinc-finger-like sequence. Proc. Natl. Acad. Sci. U. S. A. 86, 4868–4871.
Pan, Q.W., Henry, S.D., Metselaar, H.J., Scholte, B., Kwekkeboom, J., Tilanus, H.W., Janssen, H.L.A., van der Laan, L.J.W., 2009. Combined antiviral activity of interferon-alpha and RNA interference directed against hepatitis C without affecting vector delivery and gene silencing. J. Mol. Medicine Jmm 87, 713–722.
Pan, Q.W., Tilanus, H.W., Janssen, H.L., van der Laan, L.J., 2011. Impdh inhibitors mycophenolic acid and ribavirin promote the expression of interferon-stimulated genes by potentiating the activity of interferon response element. Hepatology 54, 1103a, 1103a.
Pears, C.J., Kour, G., House, C., Kemp, B.E., Parker, P.J., 1990. Mutagenesis of the pseudosubstrate site of protein-kinase-C leads to activation. Eur. J. Biochem. 194, 89–94.
Pfefferle, S., Frickmann, H., Gabriel, M., Schmitz, N., Gunther, S., Schmidt-Chanasit, J., 2012. Fatal course of an autochthonous hepatitis E virus infection in a patient with leukemia in Germany. Infection 40, 451–454.
Rask-Andersen, M., Zhang, J., Fabbro, D., Schioth, H.B., 2014. Advances in kinase targeting: current clinical use and clinical trials. Trends Pharmacol. Sci. 35, 604–620.
Robinson, J.T., Thorvaldsdottir, H., Winckler, W., Guttman, M., Lander, E.S., Getz, G., Mesirov, J.P., 2011. Integrative genomics viewer. Nat. Biotechnol. 29, 24–26.
Schaar, D., Goodell, L., Aisner, J., Cui, X.X., Han, Z.T., Chang, R., Martin, J., Grospe, S., Dudek, L., Riley, J., Manago, J., Lin, Y., Rubin, E.H., Conney, A., Strair, R.K., 2006. A phase I clinical trial of 12- O-tetradecanoylphorbol-13-acetate for patients with relapsed/refractory malignancies. Cancer Chemother. Pharmacol. 57, 789–795.
Schmieder, R., Edwards, R., 2011. Fast identification and removal of sequence contamination from genomic and metagenomic datasets. PLoS One 6, e17288.
Schrauwen, E.J., Bestebroer, T.M., Rimmelzwaan, G.F., Osterhaus, A.D., Fouchier, R.A., Herfst, S., 2013. Reassortment between Avian H5N1 and human influenza viruses is mainly restricted to the matrix and neuraminidase gene segments. PLoS One 8, e59889.
Shukla, P., Nguyen, H.T., Faulk, K., Mather, K., Torian, U., Engle, R.E., Emerson, S.U., 2012. Adaptation of a genotype 3 hepatitis E virus to efficient growth in cell culture depends on an inserted human gene segment acquired by recombination. J. Virol. 86, 5697–5707.
Shukla, P., Nguyen, H.T., Torian, U., Engle, R.E., Faulk, K., Dalton, H.R., Bendall, R.P., Keane, F.E., Purcell, R.H., Emerson, S.U., 2011. Cross-species infections of cultured cells by hepatitis E virus and discovery of an infectious virus-host recombinant. Proc. Natl. Acad. Sci. U. S. A. 108, 2438–2443.
Thorvaldsdottir, H., Robinson, J.T., Mesirov, J.P., 2013. Integrative Genomics Viewer (IGV): high-performance genomics data visualization and exploration. Brief. Bioinform. 14, 178–192.
Todt, D., Francois, C., Anggakusuma, Behrendt, P., Engelmann, M., Knegendorf, L., Vieyres, G., Wedemeyer, H., Hartmann, R., Pietschmann, T., Duverlie, G., Steinmann, E., 2016. Antiviral activities of different interferon types and subtypes against hepatitis E virus replication. Antimicrob. Agents Chemother. 60, 2132–2139.
van Bel, N., Das, A.T., Cornelissen, M., Abbink, T.E., Berkhout, B., 2014. A short sequence motif in the 5' leader of the HIV-1 genome modulates extended RNA dimer formation and virus replication. J. Biol. Chem. 289, 35061–35074.
Wang, W., Hakim, M.S., Nair, V.P., de Ruiter, P.E., Huang, F., Sprengers, D., Van Der Laan, L.J., Peppelenbosch, M.P., Surjit, M., Pan, Q., 2016a. Distinct antiviral potency of sofosbuvir against hepatitis C and E Viruses. Gastroenterology 151, 1251–1253.
Wang, W., Xu, L., Brandsma, J.H., Wang, Y., Hakim, M.S., Zhou, X., Yin, Y., Fuhler, G.M., van der Laan, L.J., van der Woude, C.J., Sprengers, D., Metselaar, H.J., Smits, R., Poot, R.A., Peppelenbosch, M.P., Pan, Q., 2016b. Convergent transcription of interferon-stimulated genes by TNF-alpha and IFN-alpha augments antiviral activity against HCV and HEV. Sci. Rep. 6, 25482.
Wang, Y.J., Zhou, X.Y., Debing, Y., Chen, K., Van der Laan, L.J.W., Neyts, J., Janssen, H.L.A., Metselaar, H.J., Peppelenbosch, M.P., Pan, Q.W., 2014. Calcineurin inhibitors stimulate and mycophenolic acid inhibits replication of hepatitis E virus. Gastroenterology 146, 1775–1783.
Wobus, C.E., Karst, S.M., Thackray, L.B., Chang, K.O., Sosnovtsev, S.V., Belliot, G., Krug, A., Mackenzie, J.M., Green, K.Y., Virgin, H.W., 2004. Replication of Norovirus in cell culture reveals a tropism for dendritic cells and macrophages. PLoS Biol. 2, e432.
Xu, L., Zhou, X., Wang, W., Wang, Y., Yin, Y., Laan, L.J., Sprengers, D., Metselaar, H.J., Peppelenbosch, M.P., Pan, Q., 2016. IFN regulatory factor 1 restricts hepatitis E virus replication by activating STAT1 to induce antiviral IFN-stimulated genes. FASEB J. 30, 3352–3367.
Zenz, R., Eferl, R., Scheinecker, C., Redlich, K., Smolen, J., Schonthaler, H.B., Kenner, L., Tschachler, E., Wagner, E.F., 2008. Activator protein 1 (Fos/Jun) functions in inflammatory bone and skin disease. Arthritis Res. Ther. 10, 201.
Zhang, B.B., Zhou, G., Li, C., 2009. AMPK: an emerging drug target for diabetes and the metabolic syndrome. Cell Metab. 9, 407–416.
Zhou, X., Xu, L., Wang, W., Watashi, K., Wang, Y., Sprengers, D., de Ruiter, P.E., van der Laan, L.J., Metselaar, H.J., Kamar, N., Peppelenbosch, M.P., Pan, Q., 2016. Disparity of basal and therapeutically activated interferon signalling in constraining hepatitis E virus infection. J. Viral Hepat. 23, 294–304.
Zhou, X.Y., Wang, Y.J., Metselaar, H.J., Janssen, H.L.A., Peppelenbosch, M.P., Pan, Q.W., 2014. Rapamycin and everolimus facilitate hepatitis E virus replication: revealing a basal defense mechanism of PI3K-PKB-mTOR pathway. J. Hepatol. 61, 746–754.